Marginality of bulk-edge correspondence for single-valley Hamiltonians

Li, Jian; Morpurgo, Alberto; Buttiker, Markus; Martin, Ivar

Marginality of bulk-edge correspondence for single-valley Hamiltonians

Jian Li,[1] Alberto F. Morpurgo,[2] Markus Büttiker,[1] and Ivar Martin[3]
[1]*Département de Physique Théorique, Université de Genève, CH-1211 Genève 4, Switzerland*
[2]*DPMC and GAP, Université de Genève, CH-1211 Genève 4, Switzerland*
[3]*Theoretical Division, Los Alamos National Laboratory, Los Alamos, New Mexico 87545, USA*
(Received 22 July 2010; revised manuscript received 2 November 2010; published 7 December 2010)

We study the correspondence between the nontrivial topological properties associated with the individual valleys of gapped bilayer graphene (BLG), as a prototypical multivalley system, and the gapless modes at its edges and other interfaces. We find that the exact connection between the valley-specific Hall conductivity and the number of gapless edge modes does not hold in general, but is dependent on the boundary conditions, even in the absence of intervalley coupling. This nonuniversality is attributed to the absence of a well-defined topological invariant within a given valley of BLG; yet, a more general topological invariant may be defined in certain cases, which explains the distinction between the BLG-vacuum and BLG-BLG interfaces.

DOI: 10.1103/PhysRevB.82.245404 PACS number(s): 73.22.Pr, 73.20.−r, 73.22.−f

I. INTRODUCTION

The analysis of the electronic properties of semiconductors often requires considering the presence in their band structure of multiple degenerate valleys, centered around different, symmetry-related positions in reciprocal space.[1] At low energy, the dynamics of electrons in each of these valleys can be modeled in terms of a long-wavelength effective Hamiltonian, an approach suitable to describe the vast majority of the transport phenomena that are measured experimentally. One interesting question—which is particularly timely in view of the intense research effort focusing on so-called topological insulators[2,3]—is whether there exist nontrivial topological properties associated to the individual valleys that can be described in the framework of a long-wavelength effective Hamiltonian.

To start addressing this question, here we focus on the case of two-dimensional electronic systems. The two best known examples of nontrivial topological insulators in two dimensions are provided by integer quantum-Hall systems[4] and by spin-orbit-induced topological insulators.[5,6] In these systems, the nontrivial topological properties of the bulk band structure result in a quantized Hall conductivity when the Fermi level is located in a bulk energy gap (for spin-orbit-induced topological insulators, spin-Hall conductivity is quantized only when the spin is a good quantum number and one can consider the Hall conductivity for each spin state separately). Indeed, it is well established that the expression of the bulk Hall conductivity σ_H given by the Kubo formula for linear response corresponds to the Chern number that characterizes the topological structure of the mapping from the Brillouin zone to the space of the Bloch states.[7,8] If we confine ourselves to the simplest case where only two bands are relevant, the physics of these systems can be described in terms of an effective Hamiltonian of the form

$$H = \sum_{\boldsymbol{k}} \Psi_{\boldsymbol{k}}^{\dagger}[-\mathbf{g}(\boldsymbol{k}) \cdot \boldsymbol{\sigma} + \epsilon_{\boldsymbol{k}} - \mu]\Psi_{\boldsymbol{k}}, \tag{1}$$

where $\Psi_{\boldsymbol{k}}=[c_{\boldsymbol{k}\uparrow}, c_{\boldsymbol{k}\downarrow}]^T$ is the itinerant electron field operator, $\boldsymbol{\sigma}=(\sigma_x, \sigma_y, \sigma_z)$ is a vector of the Pauli matrices, and $\mathbf{g}(\boldsymbol{k})$ is a real vector. If the bulk band structure is fully gapped, and the chemical potential μ lies inside the gap, the Hall conductivity (in units of e^2/h neglecting spin degeneracy), equal to the Chern number associated to the occupied band, is given by[9]

$$\sigma_H = N = \frac{1}{4\pi}\int d^2k\hat{\mathbf{g}} \cdot (\partial_{k_x}\hat{\mathbf{g}} \times \partial_{k_y}\hat{\mathbf{g}}) \tag{2}$$

with $\hat{\mathbf{g}}=\mathbf{g}/|\mathbf{g}|$ (again, for spin-orbit-induced topological insulators with conserved spin, these expressions hold separately for the two spin directions). The integral has to be performed over the entire Brillouin zone. The system is topologically nontrivial if $N \neq 0$. The physical manifestation of the topological nontriviality, which discriminates between topological and trivial insulators, is the appearance of N gapless states at the system edges, which can transport current even when the Fermi level is located in the bulk energy gap. This statement, true for both integer quantum-Hall and spin-orbit-induced topological insulators with conserved spin, relates the bulk electronic structure (which determines the Chern

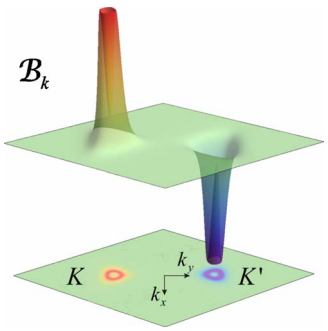

FIG. 1. (Color online) Plot of $\mathcal{B}_k=\frac{1}{4\pi}\hat{\mathbf{g}}\cdot[\partial_{k_x}\hat{\mathbf{g}}\times\partial_{k_y}\hat{\mathbf{g}}]$ [integrand of Eq. (2)] as a function of momentum $\boldsymbol{k}$ over the entire Brillouin zone, obtained from the tight-binding description of gapped BLG. $\mathcal{B}_k$ is nonvanishing only close to the K and K′ points (valleys), where it is well approximated by the expression for $\hat{\mathbf{g}}(\boldsymbol{k})$ that enters the long-wavelength effective Hamiltonian [see Eq. (6)]. The integral of $\mathcal{B}_k$ over the entire Brillouin zone vanishes, owing to the equal and opposite contributions of the two valleys ($=\pm 1$, corresponding to the quantized Hall conductivity of the individual valleys).

number) to the edge properties and is known as *bulk-edge correspondence*.[10,11]

The integrand in Eq. (2) is often sharply peaked in the regions of the momentum space where $|\mathbf{g}(\mathbf{k})|$, and hence the gap, becomes small—these are the valleys of the band structure. Thanks to the fast convergence, the integral in Eq. (2) over the Brillouin zone can be calculated using the long-wavelength approximation for the Hamiltonian valid in the individual valleys. In this case one can associate an index N_τ to each one of the valleys (τ labels the valley) and the Chern number is then the sum of the N_τ. This sum can vanish even if the individual N_τ do not, in which case the system is—according to the definition given above—topologically trivial. However, the question arises as to whether the nonvanishing of the N_τ associated to the individual valleys has observable consequences. Indeed, a nonvanishing N_τ implies that valley τ gives an nonzero contribution to the Hall conductivity and the appearance of N_τ gapless edge states associated to each individual valley may be expected by a naive "extension" of the bulk-edge correspondence. It may be argued that due to the overall triviality of the system (i.e., the fact that the Chern number defined over the entire Brillouin zone vanishes) these states localize because they are not protected against disorder at the edge, which causes intervalley scattering.[12] Nevertheless, the fundamental question remains, whether in a system with ideal edges (i.e., edges that preserve the *valley quantum number*, well defined at low energies) there exists a bulk-edge correspondence for individual valleys.

Here we consider the case of gapped bilayer graphene (BLG) as a model system for the case in which two symmetry-related valleys are present (the K and K' valleys with nonvanishing $N_\tau = \pm 1$ depending on the valley, see Fig. 1), and investigate the low-energy electronic states at its edges. Specifically, we consider different crystalline edges which do not couple the valleys, and we find the corresponding edge states in the different cases (we have discussed elsewhere the effect of disordered edges, which is experimentally more relevant[12]). If the bulk-edge correspondence could be generically extended to single-valley Hamiltonians, one would expect that $N_\tau = \pm 1$ should imply the presence of exactly one gapless mode per valley per spin at an ideal edge of gapped BLG, for all edges that do not couple the valleys. In contrast to this expectation, we show through an explicit analytical solution in complete agreement with full tight-binding calculations, that the number of the gapless edge modes depends on the boundary conditions, even when no mixing between valleys exists at the edge.[13] In other words, *the valley-specific bulk-edge correspondence is not fulfilled for plain BLG-vacuum interfaces.*

In order to understand this result, we examine the geometrical meaning of N_τ associated to a particular valley Hamiltonian, and find that, contrary to the case of the Chern numbers in topological insulators (defined over the entire Brillouin zone), N_τ in BLG does not correspond in itself to a well-defined topological invariant of a mapping. Nevertheless, the nonvanishing of N_τ still signals that the properties of the electron states in individual valleys are nontrivial, and we discuss how this nontriviality manifests itself at interfaces between different domains where the gap of BLG changes sign.[14] In this case, the number of zero-energy states corresponds to the difference of N_τ on opposite sides of the BLG-BLG interface ($N_\tau^l - N_\tau^r$, where we denote with $N_\tau^{l,r}$ the value of N_τ at the left and at the right of the BLG-BLG interface), in agreement with expectations based on bulk-edge correspondence. Indeed, we show that for a BLG-BLG interface the difference $N_\tau^l - N_\tau^r$ is a well-defined topological invariant of a mapping, even though the individual N_τ^l and N_τ^r are not. These results reveal the *marginal* character of individual valleys in gapped BLG: the *difference* of N_τ across an interface may or may not be topologically well defined, depending on the specific kind of interface. It is a well-defined topological invariant across a domain wall where the gap changes sign but it is not for a BLG-vacuum interface. Such a marginal topological character of a single valley is likely to be not only characteristic of BLG but is a more general property common to many other multivalley systems.

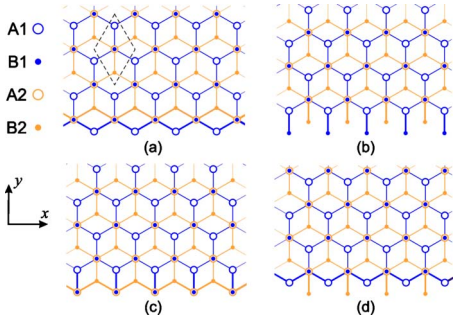

FIG. 2. (Color online) Illustration of bilayer graphene edges (highlighted by thick lines) terminating all in the zigzag direction but with different sublattices. The number of subgap edge modes is 1 for case (a) and (b), 2 for case (c), and 0 for case (d). A unit cell of the lattice is also shown in (a) in broken lines.

II. ABSENCE OF VALLEY-SPECIFIC BULK-EDGE CORRESPONDENCE

We start by briefly reviewing the known properties of the band structure of bilayer graphene, emphasizing the specific aspects that will be relevant later. In BLG a gap between valence and conductance bands can be opened controllably by applying a perpendicular electric field while maintaining the Fermi energy in the middle of the gap[15–17] (the sign of the gap is determined by the orientation of the field). The continuum low-energy, long-wavelength limit Hamiltonian for each individual valley can be obtained from the tight-binding description of BLG with Bernal stacking.[18] With the four inequivalent atoms in a unit cell labeled by $A(B)1(2)$ [see Fig. 2(a)], the dimensionless Hamiltonian matrix for the wave function $\Psi = (\chi_{B1}, \chi_{A2}, \varphi_{B2}, \varphi_{A1})^T$ reads[19]

$$H_\tau = \begin{pmatrix} H_1 & K_\tau \\ K_\tau & H_0 \end{pmatrix},$$

$$H_1 = \sigma_x + \Delta\sigma_z, \quad H_0 = -\Delta\sigma_z,$$

$$K_\tau = K_\tau^\dagger = \tau k_x \sigma_x + k_y \sigma_y. \quad (3)$$

Here, $\boldsymbol{k}=(k_x,k_y)$ is the (dimensionless) wave vector, the valley index $\tau=\pm 1$, and $2|\Delta|$ ($|\Delta| \ll 1$) defines the size of the bulk gap. The excitation spectrum is $E_{h,l} \simeq \pm\sqrt{\Delta^2+(k^2+\epsilon_{h,l}^2)^2}$, with $\epsilon_h=1$ and $\epsilon_l=0$. This implies a splitting of an order of magnitude 1 between the high-energy bands (h) and direct gap $2|\Delta|$ between the low-energy bands (l).

The original four-component Hamiltonian (3) can be inconvenient to work with, especially when one needs to find solutions with specific boundary conditions. Therefore, bearing in mind that the energy range of our interests would only involve the two low energy bands, we reduce Eq. (3) to a two-component Hamiltonian by rewriting the Schrödinger equation $H_\tau \Psi = E\Psi$ in the following form:

$$\chi = -(E+\sigma_x+\Delta\sigma_z)K_\tau \varphi, \quad (4)$$

$$-[K_\tau \sigma_x K_\tau + \Delta(1-k^2)\sigma_z]\varphi = E(1+k^2)\varphi, \quad (5)$$

where $\varphi=(\varphi_{B2},\varphi_{A1})^T$ and $\chi=(\chi_{B1},\chi_{A2})^T$. As we are interested in the subgap edge state solutions with $|E|<|\Delta| \ll 1$, only terms up to linear order in E and Δ are kept. If we further neglect $O(\Delta k^2)$ and $O(Ek^2)$ terms, we obtain

$$-\begin{pmatrix} \Delta & (\tau k_x - i k_y)^2 \\ (\tau k_x + i k_y)^2 & -\Delta \end{pmatrix}\varphi = E\varphi, \quad (6)$$

which is the reduced Hamiltonian, describing the low-energy bands to the lowest order in Δ and k. This reduction procedure is essentially identical to that used by McCann and Fal'ko.[18] Here we emphasize two important aspects: first, the nontrivial topological properties of the original four-component model are fully inherited by the reduced two-component model—this will be shown in Sec. II A; second, the relation between the low-energy (φ) and high-energy (χ) components of the wave function [Eq. (4)] is essential to impose the correct boundary conditions at edges—this will be shown in Sec. II B.

A. Quantized Hall conductivity of individual valleys

Starting from the effective Hamiltonians given previously and following the logic explained in Sec. I, we examine the nontrivial topological properties of a single valley of gapped BLG by calculating the corresponding (single-valley) contribution to the Hall conductivity σ_H^τ. We consider the case when the Fermi energy is lying in the middle of the bulk energy gap so that we are dealing with one completely full and one completely empty bulk bands of Eq. (6). The valley-specific Hall conductivity σ_H^τ (in units of e^2/h) corresponds, through Kubo formula, to the quantity N_τ defined previously. Here we present calculations for both the original four-band model, Eq. (3), and the reduced two-band model, Eq. (6), and show that these calculations yield consistent results. This consistency implies that the nontrivial momentum topology of the original four-band model is fully inherited by the two-band model, which lends itself more easily to a geometrical interpretation of our results.

The Hall conductivity (in units of e^2/h) associated to a fully gapped model is generically given by[20,21]

$$N = \frac{e_{\mu\nu\lambda}}{24\pi^2}\mathrm{Tr}\int d^2k dk_0 G\partial_{k_\mu}G^{-1}G\partial_{k_\nu}G^{-1}G\partial_{k_\lambda}G^{-1}, \quad (7)$$

where the nonsingular propagator $G(k_0,\boldsymbol{k})$ is defined as $G \equiv (ik_0-H)^{-1}$. For the four-component single-valley Hamiltonian of BLG, Eq. (3), we find $N_\tau=\tau\,\mathrm{sign}(\Delta)$, which is equal in magnitude but opposite in sign (± 1) for two valleys; therefore, the Chern number defined over the entire Brillouin zone vanishes. This result is expected for BLG, which is strictly speaking topologically trivial, despite the fact that the individual valleys possess nontrivial N_τ.

For the reduced two-component model given by Eq. (6), we can write the Hamiltonian as $H_\tau^{(2\times 2)}=-\mathbf{g}_\tau(\boldsymbol{k})\cdot\sigma$, where $\mathbf{g}_\tau(\boldsymbol{k})=(k_x^2-k_y^2, 2\tau k_x k_y, \Delta)$. In this case, using the simplified form of the above formula for two-band models,[9] given by Eq. (2), we find $N_\tau=\tau\,\mathrm{sign}(\Delta)$, in agreement with the calculation based on the full four-band model. This agreement indicates that the nontrivial topological properties of the individual valleys are due solely to the low-energy bands.

It is worth noting that the integral (divided by 2) in Eq. (2) can be also identified as the Berry phase acquired by an electron adiabatically transferred along the path enclosing the area of the integral.[22] In this sense, the quantized Hall conductivity is equivalent to the quantized Berry phase (in units of 2π) associated with the single-valley Hamiltonian.[23]

B. Boundary conditions and zero-energy edge states

We now proceed to calculate the exact solution of the edge states in gapped BLG, for different edge structures that do not mix the valleys. We will only consider one of the two valleys, with $\tau=+1$, and the results for the other valley can be inferred through a symmetry transformation similar to time reversal.

The generic constraint for boundary conditions in the present model is imposed by vanishing probability current across the boundary. This constraint allows for a variety of boundary conditions which are physically valid (see Appendix). In order to base our investigation on concrete physical examples, we illustrate the boundary conditions that will be discussed in the following in the tight-binding picture of BLG. Figure 2 shows the edge structure for four cases, where the BLG lattice terminates at different sublattices, either A or B, in each of the two layers. Indeed, each of these combinations corresponds to a distinct boundary condition imposed in the continuum model, similar in spirit to what has been discussed by Brey and Fertig[24] for single-layer graphene. A significant difference is that in BLG the boundary conditions in general involve both low (φ) and high (χ) energy components of the wave function. Still, thanks to Eq. (4), the latter can be written in terms of the low-energy components and their derivatives, which is why a description in terms of the low-energy components only is possible. For the structure in Fig. 2(a) where the BLG lattice terminates at the edge with sublattices $A1$ and $A2$, this corresponds to imposing $\varphi_{B2}(y=0)=\chi_{B1}(y=0)=0$ (the BLG is infinitely long in the x direction and semi-infinite in the $+y$ direction, i.e., the edge is located at $y=0$). The general solution of Eq. (5) for $|E|<|\Delta|$ is

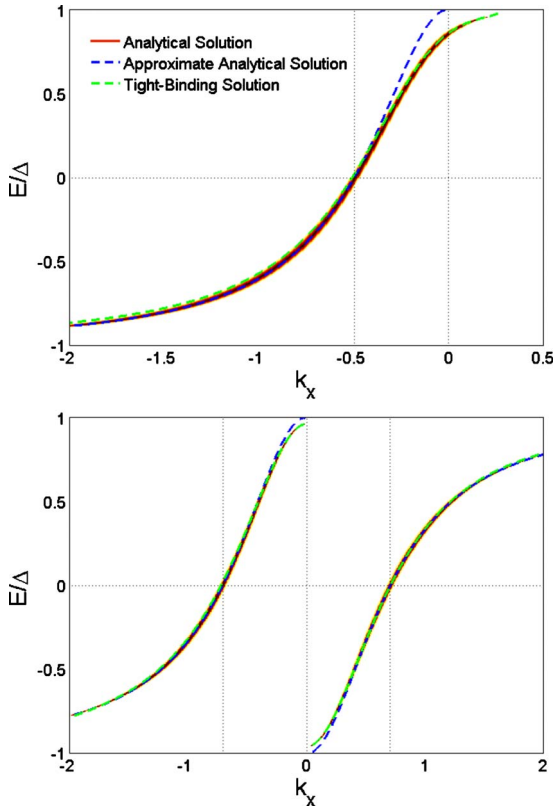

FIG. 3. (Color online) Comparison of the dispersion relations for the subgap edge modes obtained by solving the continuum model and exact diagonalization of the tight-binding model, with $\Delta=0.15$. The upper panel case corresponds to the edge shown in Fig. 2(a), and contains only one branch of gapless edge modes; the lower panel case corresponds to Fig. 2(c) and contains two branches of gapless edge modes.

$$\varphi = \sum_{s=\pm} c_s \begin{pmatrix} 1 \\ -\dfrac{(\Delta+E)-(\Delta-E)(k_x^2-\kappa_s^2)}{(k_x+\kappa_s)^2} \end{pmatrix} e^{ik_x x-\kappa_s y} \quad (8)$$

with

$$\kappa_\pm^2 = k_x^2 - (\Delta^2+E^2) \pm i\sqrt{\Delta^2-E^2}, \quad \Re(\kappa_\pm)>0, \quad (9)$$

and $c_s(s=\pm)$ are coefficients that need to be determined. Using Eq. (4), the boundary conditions lead to two coupled equations for c_s with the secular equation for the existence of nontrivial subgap solutions

$$(k_x+\kappa_+)(k_x+\kappa_-) = (\Delta+E)^2. \quad (10)$$

This equation gives the dispersion relation $E(k_x)$ for one subgap edge mode. When $|E|,|\Delta| \ll k_x^2$ (as is true for the $E=0$ mode) Eq. (10) can be simplified [since $\kappa_\pm \simeq |k_x| \pm i(\sqrt{\Delta^2-E^2})/2|k_x|$] to

$$\frac{E}{\Delta} = \frac{1-4k_x^2}{1+4k_x^2}, \quad k_x<0. \quad (11)$$

In Fig. 3(a) the analytical solution is compared with the full tight-binding solution, from which we see that the continuum model represents an excellent approximation. We conclude that for the edge just considered, one zero mode exists (per valley and spin),[25] i.e., the result expected if the bulk-edge correspondence for single valley holds.

We now consider the edge shown in Fig. 2(c). The corresponding boundary conditions are $\varphi_{B2}(y=0)=\varphi_{A1}(y=0)=0$, which lead to the new dispersion relation for the subgap edge modes, given by

$$\frac{2k_x(k_x+\kappa_+)(k_x+\kappa_-)}{2k_x+\kappa_++\kappa_-} = \frac{\Delta+E}{\Delta-E}. \quad (12)$$

This equation has two solutions related by transformation $k_x \to -k_x$ and $E \to -E$, which comes from the symmetry of the wave Eq. (5) under $\{k_x,E,\varphi\} \to \{-k_x,-E,i\sigma_y\varphi\}$. It is this symmetry, which is also preserved by the boundary conditions in the present case (whereas it is broken by the boundary conditions considered in the previous example), that guarantees the existence of *two* subgap edge modes. The dispersion relation given by Eq. (12) can be further simplified when $|E|,|\Delta| \ll k_x^2$, to

$$\frac{E}{\Delta} = -\,\mathrm{sgn}(k_x)\frac{1-2k_x^2}{1+2k_x^2}, \quad (13)$$

which explicitly shows a pair of gapless edge modes propagating in the same direction, plotted in Fig. 3(b) (again, in excellent agreement with the tight-binding solution). Without presenting the details of the solutions for the other cases, we only state that the edge shown in Fig. 2(b) $[\varphi_{A1}(y=0)=\chi_{A2}(y=0)=0]$ leads to a single branch of subgap edge modes, similar to the first example above, and the one shown in Fig. 2(d) $[\chi_{B1}(y=0)=\chi_{A2}(y=0)=0]$ yields no subgap modes. We therefore have to conclude that the number of zero modes at the BLG-vacuum interface depends on the specific edge considered, i.e., the bulk-edge correspondence relating the Hall conductivity and gapless edge modes does not hold in general for individual valleys.[26]

III. DISCUSSION

Finding that bulk-edge correspondence does not hold for an individual valley, even though the contribution that each valley gives to the Hall conductivity is integer (in units of e^2/h) may seem surprising. Specifically, one may wonder why the argument based on Laughlin's gedanken experiment[27]—which is normally invoked to justify the existence of edge states in integer quantum-Hall systems—does not apply to individual valleys in gapped BLG. The answer to this question has to do with the fact that Laughlin's gedanken experiment considers the adiabatic flow of electric charge, which is a conserved quantity (in the context of Laughlin's argument conservation of charge is so obvious that this assumption is not normally emphasized). Contrary to the charge, the valley quantum number is not in general conserved. In particular, it is not conserved even in the presence of ideal edges if one considers the process—the adiabatic insertion of flux—which is the basis of Laughlin's gedanken experiment. As we outline below, the nonconservation of the valley quantum number allows for the possibility of a quantized valley Hall conductivity in the absence of zero-energy edge modes.

Upon varying the magnetic flux ϕ in the usual cylindrical geometry involved in Laughlin's argument, the allowed k_x values of momentum along the edge flow according to $k_x \rightarrow k_x + \phi/L$, where L is the circumference of the cylinder. Upon insertion of flux $\phi = 2\pi$, the set of allowed k_x values returns to the original one. From the generic form of the electron wave function, Eq. (8), it follows that the wave-function weight is redistributed in the direction perpendicular to the edge in the process of flux insertion. The redistribution occurs in the opposite directions for the states near two valleys, with states in one valley flowing toward the edge, and states in the other valley flowing away from the edge. This is the microscopic mechanism for the transverse valley current flow implied by the nonzero value of the valley Hall conductivity, $\sigma_H^v = N_\tau - N_{-\tau}$. The fact that the valley current flows perpendicular to the edge, according to continuity equation would imply accumulation of the valley density at the edge. This apparent valley charge accumulation can be accommodated in two ways. The first is by creating valley charge imbalance at the edge, in direct analogy to quantum-Hall and quantum spin-Hall effect with conserved spin. Clearly, for that to occur, the gapless edge modes have to exist. Alternatively, the valley current influx at the edge can be compensated by the adiabatic transfer of the electrons between the valleys induced by the flux insertion, which converts $k_x \rightarrow k_x + 2\pi/L$ for states in the *entire* one-dimensional (1D) Brillouin zone of the cylinder. This is possible due to the fact that the valleys are indeed connected by the bands that extend deep below the chemical potential. As a consequence, the spectral flow cannot be fully described in terms of the long-wavelength effective Hamiltonian in the neighborhood of the K and K′ points but it requires considering the Hamiltonian of the system over the entire Brillouin zone. This is how the nonconservation of the valley quantum number can account for the seemingly paradoxical result that nonzero σ_H^v can exist even when gapless edge modes are completely absent.[28]

Next, let us give a geometrical reason for the absence of a valley-specific bulk-edge correspondence at gapped BLG edges (BLG-vacuum interfaces). It originates from the fact that the quantity N_τ associated with a given valley is not a well-defined topological invariant. This statement may appear to be in conflict with the case of domain-wall interfaces, across which the sign of the mass (Δ) in BLG changes sign.[14] In this latter case, bulk-edge correspondence "predicts" that gapless states should be present, whose number corresponds to $N_\tau^l - N_\tau^r$. When the gap Δ changes sign across the domain wall, $|N_\tau^l - N_\tau^r| = 2$ and indeed two gapless states are found at the interface. The conflict is only apparent, because $N_\tau^l - N_\tau^r$ does correspond to a well-defined topological invariant, even though N_τ does not.

To understand the difference between N_τ and $N_\tau^l - N_\tau^r$ we look at the integrand function that is used to calculate these quantities, which, from Eq. (2), is given by $\mathcal{B}_k = \frac{1}{4\pi}\hat{\mathbf{g}} \cdot [\partial_{k_x}\hat{\mathbf{g}} \times \partial_{k_y}\hat{\mathbf{g}}]$. This expression corresponds to the Jacobian of the transformation from the region R^2 of the momentum space in the vicinity of a given valley point, to the unit sphere S^2 on which $\hat{\mathbf{g}}$ resides. For BLG, at large $k (k^2 \gg |\Delta|)$, the vector $\hat{\mathbf{g}}$ lies on the equator, and therefore the integral of $\mathcal{B}_k$ does not represent a topological invariant since the mapping between noncompact R^2 and compact S^2 is topologically trivial. Indeed, as shown in Figs. 4(a) and 4(b), the vector $\hat{\mathbf{g}}$ wraps around half of the unit sphere twice, but does not cover the entire sphere. That is despite the fact that the integral rapidly converges for $k^2 \gg |\Delta|$ and is equal to 1 (for a given valley and sign of the gap Δ; it is -1 for the opposite valley or for opposite sign of Δ). For massive Dirac fermions such noncompact behavior has been discussed by Volovik, and is known as *marginal*.[9] In the same sense, the massive chiral fermions in BLG are marginal as well. The marginality implies that a small perturbation in the Hamiltonian [e.g., momentum-dependent mass term $\Delta(k^2)$] or boundary conditions can have a big effect on presence or absence of the gapless modes (e.g., Ref. 29).

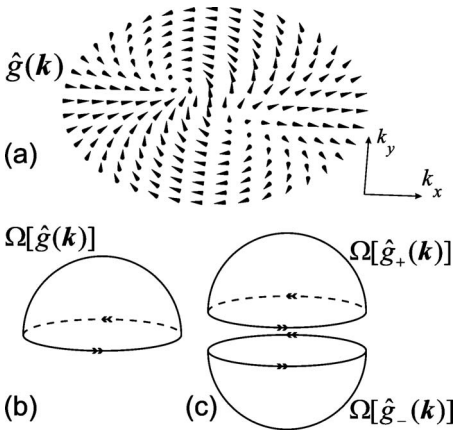

FIG. 4. Illustration of the mapping $\hat{\mathbf{g}}(\boldsymbol{k})$ for gapped BLG. Panel (a) shows $\hat{\mathbf{g}}(\boldsymbol{k})$ for a single valley as a vector field on the R^2 plane of $\boldsymbol{k}$. Panel (b) shows the solid angle Ω that $\hat{\mathbf{g}}$ covers when $\boldsymbol{k}$ runs over the whole plane, the double arrow signifying the double covering of the (upper) hemisphere. Panel (c) shows how two marginal topological mappings can be "glued" to form a well-defined topological mapping, which is the case for a BLG-BLG domain wall with opposite mass signs on the two sides.

Now, for a domain wall such that $\Delta(x<0)<0$ and $\Delta(x>0)>0$, despite the marginal character of N_τ on the two sides of the domain wall, their difference is a well-defined topological invariant. That is because at $k \rightarrow \infty$, the Δ in the Hamiltonians becomes irrelevant and the textures of the $\hat{\mathbf{g}}$ vectors for the two insulators seamlessly connect on the equator of S^2, thereby compactifying the momentum space *within the same valley*. The connection of the textures is shown schematically in Fig. 4(c). Similar considerations are not only valid for BLG, but can also be extended to individual valleys in (gapped) single-layer graphene,[30] as well as to interfaces between gapped single-layer graphene and Kane-Mele topological insulators with conserved spin.[5] In these cases, the differences in the single-valley N_τ across the interface is a well-defined topological invariant, corresponding to number of gapless states present (or more precisely, the difference between the numbers of left and right moving gapless modes in a given valley). Mathematically, this is a consequence of the index theorem discussed in this type of contexts by Volovik (see Section 22.1.4 in Ref. 9).

IV. CONCLUSION

Our work shows that the long-wavelength Hamiltonians that describe the low-energy electronic states in individual valleys of gapped BLG possess nontrivial topological features. In contrast to integer quantum-Hall systems and quantum spin-Hall systems (with conserved spin), these nontrivial valley-specific properties cannot be described by a topological invariant. Rather, they require the analysis of the specific interfaces (in the present case the BLG-vacuum interface and the domain wall) in order to establish whether a topological invariant that determines the number of gapless edge modes can be defined. This is the characteristic signature of marginal topological insulators.

It is certainly the case that the low-energy edge states that can be predicted through these topological considerations are not robust against short-range disorder that couples the valleys (even though they are stable against long-range disorder that scatters electrons within the same valley). In the presence of intervalley scattering, the gapless modes associated to individual valleys will couple, leading to the opening of a transport gap. Nevertheless, this does not mean that the low-energy states at interfaces and domain walls are experimentally irrelevant. In fact, for sufficiently pure materials when the Fermi energy is in the gap, the states originating from the localization of the gapless modes can provide a dominant path for transport in the insulating state, because no other states are available deep in the bulk gap of the material.[12]

Finally, even though all calculations presented here have been performed specifically for gapped BLG, our arguments do not rely on the particular form of the valley Hamiltonian, or the number of valleys. Consequently, similar treatment based on other effective valley Hamiltonians should be applicable to many other materials and interfaces and may provide a convenient tool for determining the interfacial electronic properties.

ACKNOWLEDGMENTS

This work has been supported by the Swiss National Science Foundation (Projects No. 200020-121807 and No. 200021-121569), by the Swiss Center of Excellence MaNEP, and the European Network NanoCTM. The work of I.M. was carried out under the auspices of the National Nuclear Security Administration of the U.S. Department of Energy at Los Alamos National Laboratory under Contract No. DE-AC52-06NA25396 and supported by the LANL/LDRD Program.

APPENDIX: BOUNDARY CONDITIONS

In this appendix we derive the most general boundary conditions from the continuum model given by Eq. (3) and (6), by imposing current conservation through a hard-wall boundary. We show that the boundary conditions associated to the edge structures considered in the main text are specific realization of the general case.

Let us start from the original four-component model, Eq. (3), for which the current operator is given by

$$\mathbf{j} = \begin{pmatrix} 0 & \boldsymbol{\sigma} \\ \boldsymbol{\sigma} & 0 \end{pmatrix}, \tag{A1}$$

where $\boldsymbol{\sigma} \equiv (\sigma_x, \sigma_y)$ and we have let $\hbar = 1$. Without losing generality, we consider a boundary at $y=0$ with unit normal $\boldsymbol{n}_B = -\hat{y}$; then, the current conservation implies

$$\Psi^\dagger (\boldsymbol{j} \cdot \boldsymbol{n}_B) \Psi|_{y=0} = i(\chi^*_{B1}\varphi_{A1} - \chi^*_{A2}\varphi_{B2})|_{y=0} + \text{c.c.} = 0. \tag{A2}$$

We immediately see that the above condition can be naturally satisfied by letting in each layer the wave amplitude on either A or B component vanish at $y=0$. This leads to four choices of combinations each finding an exact correspondence to the cases listed in Fig. 2. Indeed, the same amount of freedom in "choosing" boundary conditions is also inherited by the reduced model, Eq. (6), for which, by the same token, the vanishing current across the boundary requires

$$(\varphi^*_{A1}\partial_+\varphi_{B2} - \varphi^*_{B2}\partial_-\varphi_{A1})|_{y=0} + \text{c.c.} = 0, \tag{A3}$$

where $\partial_\pm \equiv \partial_x \pm i\partial_y$. Noticing that the leading-order approximation of Eq. (4) yields

$$\chi_{B1} = i\partial_+\varphi_{B2}, \quad \chi_{A2} = i\partial_-\varphi_{A1}, \tag{A4}$$

Equation (A3) is nothing but Eq. (A2). In other words, the reduced model shares the same choices of boundary conditions as the original one, and the edge modes it allows for, may vary accordingly.

These derivations indicate that for a generic multicomponent Hamiltonian, considerable freedom exist in selecting boundary conditions associated to the wave equation, reflecting different possible structures of the edges. To demonstrate the dependence of the gapless edge modes on boundary conditions, which serves the purpose of the current work, however, the four cases presented in the main text are already sufficient.

[1] K. Seeger, *Semiconductor Physics: An Introduction*, 5th ed. (Springer, Berlin, 1991).
[2] M. Hasan and C. Kane, Rev. Mod. Phys. **82**, 3045 (2010).
[3] X.-L. Qi and S.-C. Zhang, Phys. Today **63**(1), 33 (2010).
[4] K. v. Klitzing, G. Dorda, and M. Pepper, Phys. Rev. Lett. **45**, 494 (1980).
[5] C. L. Kane and E. J. Mele, Phys. Rev. Lett. **95**, 226801 (2005).
[6] B. A. Bernevig, T. L. Hughes, and S.-C. Zhang, Science **314**, 1757 (2006).
[7] D. J. Thouless, M. Kohmoto, M. P. Nightingale, and M. den Nijs, Phys. Rev. Lett. **49**, 405 (1982).
[8] M. Kohmoto, Ann. Phys. **160**, 343 (1985).
[9] G. Volovik, *The Universe in a Helium Droplet* (Oxford University Press, New York, 2003).
[10] Y. Hatsugai, Phys. Rev. Lett. **71**, 3697 (1993).
[11] X.-L. Qi, Y.-S. Wu, and S.-C. Zhang, Phys. Rev. B **74**, 045125

(2006).
[12] J. Li, I. Martin, M. Buttiker, and A. F. Morpurgo, Nat. Phys., doi:10.1038/nphys1822 (2010).
[13] It is interesting to note that in the presence of edge disorder in gapped BLG the universal connection between the quantized Hall conductivity and the number of edge modes is reinstated: the subgap transport is dominated by the edge conductance that corresponds to a single 1D channel per spin with long localization length (Ref. 12).
[14] I. Martin, Y. M. Blanter, and A. F. Morpurgo, Phys. Rev. Lett. **100**, 036804 (2008).
[15] E. V. Castro, K. S. Novoselov, S. V. Morozov, N. M. R. Peres, J. M. B. Lopes dos Santos, J. Nilsson, F. Guinea, A. K. Geim, and A. H. Castro Neto, Phys. Rev. Lett. **99**, 216802 (2007).
[16] J. B. Oostinga, H. B. Heersche, X. Liu, A. F. Morpurgo, and L. M. K. Vandersypen, Nature Mater. **7**, 151 (2008).
[17] Y. Zhang, T. Tang, C. Girit, Z. Hao, M. C. Martin, A. Zettl, M. F. Crommie, Y. R. Shen, and F. Wang, Nature (London) **459**, 820 (2009).
[18] E. McCann and V. I. Fal'ko, Phys. Rev. Lett. **96**, 086805 (2006).
[19] To make the Hamiltonian and all its parameters dimensionless, we scale energy with $t_\perp$ and wave vector with $1/l_0 \equiv 2t_\perp/3ta$, where $t_\perp$ is the interlayer hopping energy, and a and t are the intralayer nearest-neighbor distance and hopping energy.
[20] G. Volovik, Sov. Phys. JETP **67**, 1804 (1988).
[21] V. M. Yakovenko, Phys. Rev. Lett. **65**, 251 (1990).
[22] D. Xiao, M. Chang, and Q. Niu, Rev. Mod. Phys. **82**, 1959 (2010).
[23] K. S. Novoselov, E. McCann, S. V. Morozov, V. I. Fal'ko, M. I. Katsnelson, U. Zeitler, D. Jiang, F. Schedin, and A. K. Geim, Nat. Phys. **2**, 177 (2006).
[24] L. Brey and H. A. Fertig, Phys. Rev. B **73**, 235411 (2006).
[25] E. V. Castro, N. M. R. Peres, J. M. B. Lopes dos Santos, A. H. Castro Neto, and F. Guinea, Phys. Rev. Lett. **100**, 026802 (2008).
[26] Similarly, there is no correspondence between the Hall conductivity and the edge modes in gapped single-layer graphene. In fact, there is a close connection between the edge states in a graphene single layer and its bilayer, as the latter can be obtained by considering two decoupled single layers, upon turning on $t_\perp$.
[27] R. B. Laughlin, Phys. Rev. B **23**, 5632 (1981).
[28] I. Martin (unpublished).
[29] W. Yao, S. A. Yang, and Q. Niu, Phys. Rev. Lett. **102**, 096801 (2009).
[30] G. W. Semenoff, V. Semenoff, and F. Zhou, Phys. Rev. Lett. **101**, 087204 (2008).